Attenuating surface gravity waves with mechanical metamaterials

Attenuating surface gravity waves with mechanical metamaterials

Cite as: Phys. Fluids **33**, 047113 (2021); https://doi.org/10.1063/5.0048613
Submitted: 24 February 2021 . Accepted: 25 March 2021 . Published Online: 26 April 2021

F. De Vita, F. De Lillo, F. Bosia, and M. Onorato

Physics of Fluids ARTICLE scitation.org/journal/phf

Attenuating surface gravity waves with mechanical metamaterials

Cite as: Phys. Fluids 33, 047113 (2021); doi: 10.1063/5.0048613
Submitted: 24 February 2021 · Accepted: 25 March 2021 ·
Published Online: 26 April 2021

F. De Vita,[1,a)] F. De Lillo,[2] F. Bosia,[3] and M. Onorato[2]

AFFILIATIONS

[1]Dipartimento di Meccanica, Matematica e Management, Politecnico di Bari, Via Orbona 4, 70125 Bari, Italy
[2]Dipartimento di Fisica and INFN, Università degli Studi di Torino, Via Pietro Giuria 1, 10125 Torino, Italy
[3]DISAT, Politecnico di Torino, Corso Duca degli Abruzzi 24, 10129 Torino, Italy

[a)]Author to whom correspondence should be addressed: francesco.devita@poliba.it

ABSTRACT

Metamaterials and photonic/phononic crystals have been successfully developed in recent years to achieve advanced wave manipulation and control, both in electromagnetism and mechanics. However, the underlying concepts are yet to be fully applied to the field of fluid dynamics and water waves. Here, we present an example of the interaction of surface gravity waves with a mechanical metamaterial, i.e., periodic underwater oscillating resonators. In particular, we study a device composed of an array of periodic submerged harmonic oscillators whose objective is to absorb wave energy and dissipate it inside the fluid in the form of heat. The study is performed using a state-of-the-art direct numerical simulation of the Navier–Stokes equation in its two-dimensional form with free boundary and moving bodies. We use a volume of fluid interface technique for tracking the surface and an immersed boundary method for the fluid–structure interaction. We first study the interaction of a monochromatic wave with a single oscillator and then add up to four resonators coupled only fluid-mechanically. We study the efficiency of the device in terms of the total energy dissipation and find that by adding resonators, the dissipation increases in a nontrivial way. As expected, a large energy attenuation is achieved when the wave and resonators are characterized by similar frequencies. As the number of resonators is increased, the range of attenuated frequencies also increases. The concept and results presented herein are of relevance for coastal protection applications.

I. INTRODUCTION

In recent years, the field of mechanical metamaterials and phononic crystals has seen a rapid development and captured increasing interest.[1] These are engineered materials that have been developed to alter the standard properties of wave propagation such as dispersion, refraction, or diffraction. Metamaterials are usually arranged in periodic patterns, at scales that are comparable or smaller than the wavelengths of the phenomena they influence. The simplest effect is that when waves propagate in a periodic structure, the dispersion relation displays banded structures with frequency regions that are forbidden, called bandgaps. This effect, for example, can be obtained in phononic biatomic materials.[2] The concept of metamaterials was first developed in the field of optics[3] and later extended to phononic crystals and elastic waves.[2] Some work on the interaction of gravity waves with a macroscopic periodic structure (a sinusoidal floor) has already been presented in the past (see Refs. 4 and 5). Results indicated the existence of a mechanism of resonant Bragg reflection occurring when the wavelength of the bottom undulation is one-half the wavelength of the surface wave. Further studies on the interactions of waves with periodic structures can be found in Refs. 6–8. Other examples of wave manipulation properties, for example cloaking, can be obtained by employing an engineered elastic buoyant carpet placed on water[9] or by a radial arrangment of vertical cylinders.[10]

The interaction of ocean waves with solid structures is a long-standing problem in fluid mechanics.[11] A theoretical approach based on the direct use of the equations of motion, even in their simplified version, is not always feasible, especially when geometries are not simple and bodies are moving because of hydrodynamical forces. In the latter cases, an experimental approach is often impractical, as the measurement of pressures and of the velocity field around the moving bodies may not be straightforward. Numerical methods, despite their complexity, offer an important alternative to study wave–structure interaction and to design structures. With respect to standard fluid mechanics, the main complication that arises is due to the presence of

a free surface which substantially increases the difficulty of the numerical treatment. Some studies in the literature assume that the flow is irrotational and inviscid so that the potential flow equations can be solved and forces are limited to pressure.[12,13] However, when the goal is to study the overall effect of wave attenuation and the energy dissipated in the bulk of the fluid, vorticity and viscosity cannot be neglected, and the full Navier–Stokes equations need to be computed: recent works[14,15] have provided evidence that viscosity plays an important role, especially close to resonant conditions. To this end, direct numerical simulation (DNS) of a free surface flow interacting with a structure represents a powerful tool that can provide a detailed representation of the flow field and of the fluid–structure interaction.

In this work, we consider the interaction of gravity waves with a periodic structure composed of "internal" resonators, i.e., waves interact with submerged harmonic oscillators which are coupled only fluid-mechanically. To begin with, we work in a two-dimensional framework; therefore, strictly speaking, our waves are characterized by infinitely long crests and the oscillators are cylinders whose axes are parallel to the crests. We solve the full Navier–Stokes system of equations coupled with the volume of fluid (VoF) method for the interface tracking and the immersed boundary method (IBM) for the fluid– structure interaction. The cylinders undergo the hydrodynamic forces (pressure and viscous stress) of the wave motion and an elastic force that tends to restore the system back to the equilibrium position. The analysis has been conducted for a variable number of resonators per wavelength and changing their natural frequency. It is worth mentioning that the system we are considering is similar to systems for wave energy conversion, on which there is a rich literature ranging from point-absorbers[15–17] to full modeling of the solid structure.[12,18] However, the focus here is on the interaction of a wave with a periodic structure rather than on the conversion of energy from a single oscillator.

II. METHODOLOGY

A. The numerical method

We solve the full Navier–Stokes system of equations:

$$\rho(\partial_t \mathbf{u} + \mathbf{u}\cdot\nabla\mathbf{u}) = -\nabla p + \nabla\cdot(\mu\mathbf{D}) + \rho\mathbf{g} + \mathbf{f}, \tag{1}$$

$$\nabla\cdot\mathbf{u} = 0, \tag{2}$$

with $\mathbf{u} = (u, w)$ the velocity field, p the pressure field, $\mathbf{D}$ the deformation tensor defined as $D_{ij} = (\partial_i u_j + \partial_j u_i)/2$, $\mathbf{g}$ the gravity vector and $\mathbf{f}$ the IBM force which enforces the no-slip boundary condition at the solid boundary. The material properties ρ and μ are related to the volume fraction field $\mathscr{F}(\mathbf{x}, t)$ as

$$\rho(\mathscr{F}) = \mathscr{F}\rho_1 + (1-\mathscr{F})\rho_2, \tag{3}$$

$$\mu(\mathscr{F}) = \mathscr{F}\mu_1 + (1-\mathscr{F})\mu_2, \tag{4}$$

where ρ_1, ρ_2, μ_1, and μ_2 are the density and viscosity of the two fluids; the volume fraction field (defined as the volumetric ratio of the two fluids in each computational cell) is advected by the flow with the following equation:

$$\partial_t\mathscr{F} + \nabla\cdot(\mathscr{F}\mathbf{u}) = 0. \tag{5}$$

The motion of the resonators is given by Newton's law

$$m_i\frac{d^2X_i}{dt^2} + \kappa_i(X_i - X_{0,i}) = F_i, \tag{6}$$

where X_i is the position of the center of mass of the ith resonator, m_i its mass, κ_i is the elastic constant, $X_{0,i}$ the equilibrium position and F_i the integral of the hydrodynamic forces acting on it. This force is computed by integrating the pressure (p) and the viscous stress tensor ($\boldsymbol{\tau}$) over the surface of the solid body as follows:

$$\mathbf{F} = \int_S (\boldsymbol{\tau} - p\mathbf{I})\cdot\mathbf{n}dS. \tag{7}$$

By computing the force in this way, all terms typically used in the description of point-absorbers (such as viscous damping and radiation damping) are included, and Eq. (7) provides a more general and accurate description of the solid body motion.

Modeled in this way, the resonator has a natural frequency $\omega_r = \sqrt{k/m}$. In the real system, resonators would correspond to reversed pendula anchored at the bottom; for waves of small amplitude, as in this study, the vertical motion of the resonators can be neglected, hence, we solve Eq. (6) only for the horizontal motion, with F_i being the horizontal component of the integral of the hydrodynamic loads acting on the ith resonator; the motion in the vertical direction is set to zero.

The Navier–Stokes equations are advanced in time using a second-order Adams–Bashforth scheme and a fractional step method is employed[19] for the coupling with the pressure; the resulting Poisson equation for the pressure is solved employing a Fast Direct Solver. All derivatives are discretized with a second-order central difference scheme apart for the diffusion term in the Navier–Stokes equations, for which a WENO scheme is used.[20] The IBM is implemented using the direct forcing approach[21] with interpolations performed in the direction normal to the interface. For the fluid–structure interaction, a strong coupling is adopted with an iterative solver based on the Hamming method.[22] The solver is limited to non-deformable solid bodies, which allows for more efficient computations. A detailed description of the solver with validations and preliminary results can be found in Ref. 23. A sketch of the periodic structure of four resonators immersed in a fluid and forced by surface gravity waves is shown in Fig. 1.

B. Initial conditions

The initial wave profile $\boldsymbol{\eta}$ and velocity field $\mathbf{u} = (u, w)$ are taken from linear theory and are, respectively,

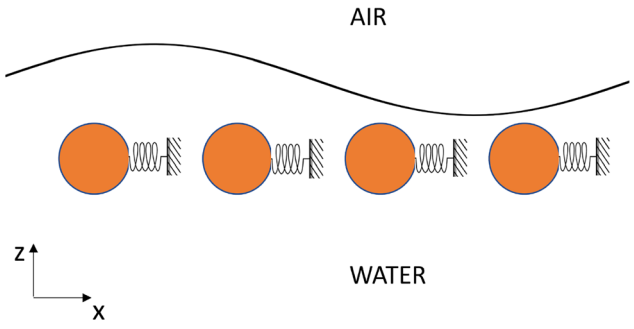

FIG. 1. Sketch of the periodic structure of resonators interacting with a surface gravity wave.

$$\eta(x,0) = a\cos(kx), \tag{8}$$

and

$$u(x,0) = a\omega e^{kz}\cos(kx), \tag{9}$$

$$w(x,0) = a\omega e^{kz}\sin(kx), \tag{10}$$

with a the wave amplitude, $k = 2\pi/\lambda$ the wavenumber, λ the wavelength and $z = 0$ the still water level, and z pointing upward. The wave frequency ω is given by the dispersion relation for water waves in deep water $\omega = \sqrt{gk}$. The initial velocity field in air is equal to that in water with the horizontal component u having a negative sign. To avoid high shear stress across the interface at the beginning of the simulation, the initial volume fraction is filtered with a bilinear interpolation which results in a spread of the interface over three cells. Note that this operation is performed only for the initial profile. The computational domain is a square of lateral size λ, the radius of the resonators is $r = 0.057\lambda$, and the distance from the center of mass of the resonators and the still water level is $d = 0.094\lambda$. The Reynolds number based on the wavelength and phase speed is set to $Re = \rho g^{1/2}\lambda^{3/2}/\mu = 10^5$, with ρ and μ the density and viscosity of the high-density phase. All simulations are performed with a grid of 512×512 computational nodes.

We performed simulations for different numbers of resonators per wavelength and different values of the ratio $\Omega = \omega_r/\omega$. The different cases are studied by changing the proper frequency and number of the oscillators, while keeping the amplitude and the length of the initial sinusoidal wave unchanged. This choice prevents *a priori* any change in the wave steepness, which would in turn affect the nonlinearity of the wave dynamics.

III. RESULTS

We first consider a single resonator placed at the center of the domain where a monochromatic wave of wavelength $\lambda = 1$ (in nondimensional units) propagates. In Fig. 2 we report snapshots of the horizontal velocity component u, the interface location and the oscillator position for the case $\Omega = 1$ at four instants of time, $t/T = 0.5, 1, 1.5, 2$, with T the wave period. Wave motion forces the resonator to move due to the pressure and viscous stress distribution; the resonator, then, is pulled back to its original position by the elastic force and starts to oscillate around its equilibrium position. This motion induces perturbations on the interface, clearly visible at a later

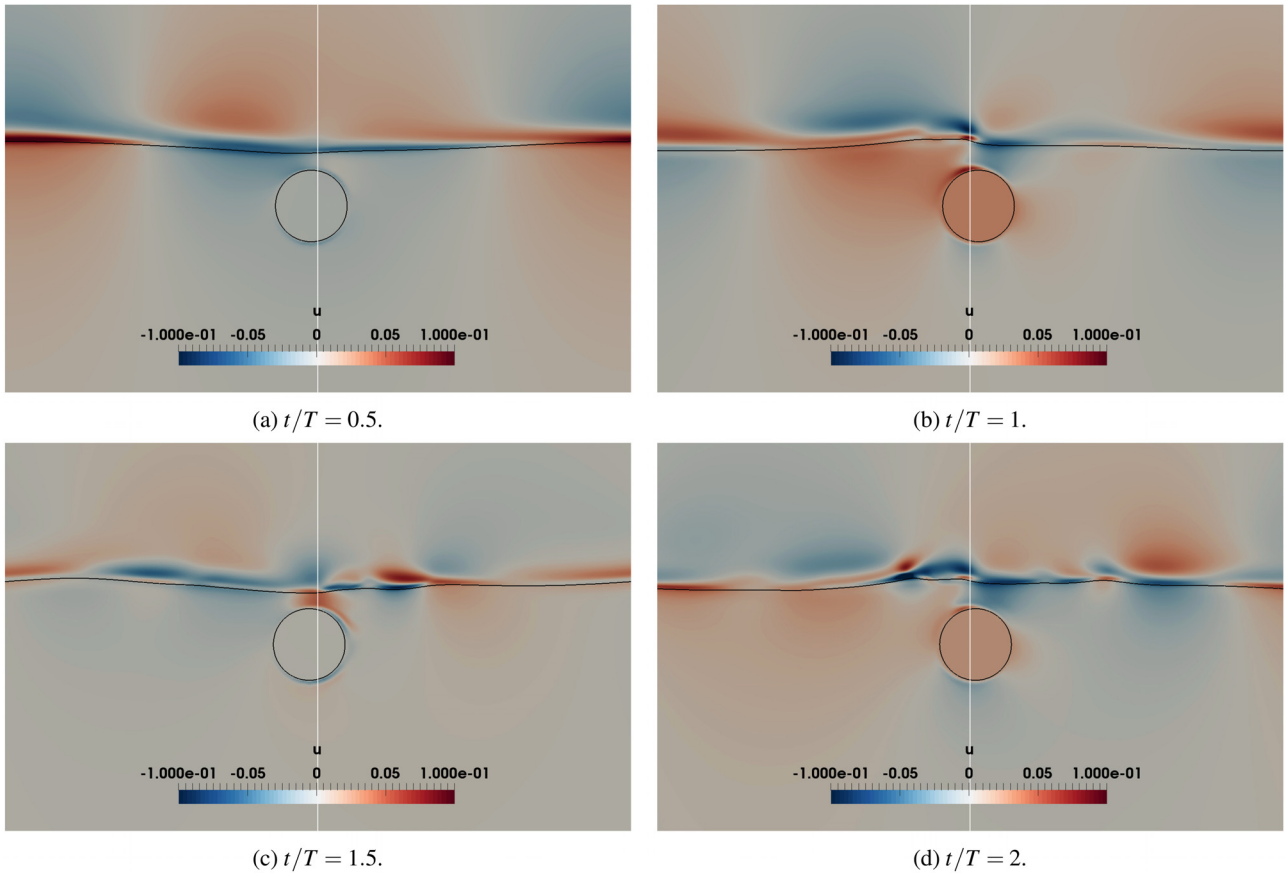

(a) $t/T = 0.5$. (b) $t/T = 1$.

(c) $t/T = 1.5$. (d) $t/T = 2$.

FIG. 2. Snapshot of the horizontal component u of the velocity field at four instants of time for the case with $\Omega = 1$. The vertical white line is located at the center of the domain and it is reported as reference to underline the motion of the resonator (multimedia view: https://doi.org/10.1063/5.0048613.1).

stage of the process [Fig. 2(d)], leading to vorticity production at the surface, which enhances the energy dissipation.

In Fig. 3 we show the time history of the displacement of the center of mass of the resonator for $\Omega = 1$, i.e., when the frequency of the wave is equal to the frequency of the resonator, and for $\Omega = 0.25$, i.e., the frequency of the wave is four times the frequency of the resonator. In one period, the wave has traveled the full domain. Due to the periodic boundary conditions, the wave re-enters the domain from the left with a reduced amplitude, both because of its natural decay due to viscosity and because of the interaction with the resonators. Therefore, the resonator oscillates with a decreasing amplitude (as highlighted in Fig. 3), since it is forced by waves whose amplitude is decreasing in time. In the inset of the figure, we plot the wave amplitude (computed as the difference between the maximum and minimum value of the surface elevation) vs time for the same cases: the simulation with $\Omega = 1$ exhibits a stronger decrease in wave amplitude which is in line with an increase in dissipation, as discussed below.

We find very instructive to show the space–time plots of the surface elevation, displayed in Fig. 4. The presence of the resonator induces a local perturbation of the surface elevation; this is clearly visible in the top panel of Fig. 4, corresponding to the case with a fixed cylinder located at $x/\lambda = 0.5$. Additionally, when the solid body oscillates, the interaction with the propagating surface gravity wave leads to the generation of a wave traveling in the opposite direction with respect to the original one. This is highlighted in the middle panel of Fig. 4 by a brown line. For this simulation, the period of the resonator is four times the wave period ($\Omega = 0.25$) and after approximately four nondimensional time intervals, there is an inversion of the direction of propagation of the wave, which is again recovered after four more wave periods. For the case $\Omega = 1$, bottom panel of Fig. 4, a similar dynamics takes place on a shorter timescale but the evolution of the free-surface is less regular.

In the following, we will quantify the dissipated power during the wave propagation as a function of Ω and of the number of resonators per wavelength. Due to the nonstationary nature of the system, these quantities must be described in a time-dependent fashion. When a

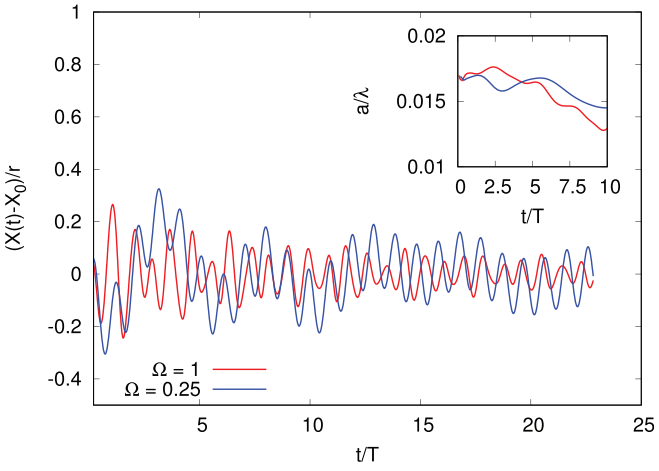

FIG. 3. Time history of the center of mass displacement of one resonator placed in the middle of the domain for two different values of Ω; the inset shows the wave amplitude vs time for the same cases.

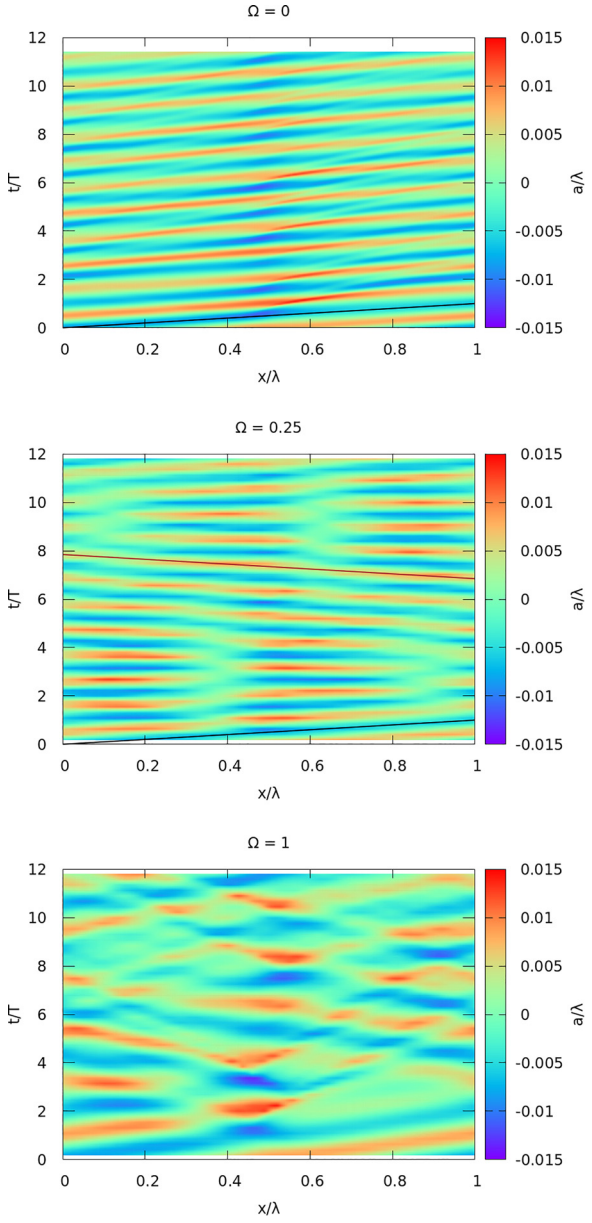

FIG. 4. Space–time evolution of the surface elevation: (top) $\Omega = 0$; (middle) $\Omega = 0.25$; and (bottom) $\Omega = 1$. The two lines in the middle panel highlight forward (black line) and backward (brown line) propagating waves.

surface gravity wave of small amplitude (i.e., small steepness $\varepsilon = ak$) propagates freely, its total energy decays with an exponential rate equal to $E(t) = E(0)e^{-2\gamma t}$, as described by Landau and Lifshitz.[24] Here, the wave energy $E(t)$ is the sum of the kinetic and potential contribution defined as

$$E(t) = K(t) + U(t) = \frac{1}{2}\int_0^{\lambda}\int_{-h}^{\eta}\rho|\mathbf{u}|^2 dzdx + \int_0^{\lambda}\int_{-h}^{\eta}\rho g z dzdx - \bar{U}, \tag{11}$$

where $z = -h$ is the position of the flat bottom, $z = \eta(x, t)$ is the displacement of the surface with respect to its equilibrium position and $\bar{U} = \int_0^{\lambda} \int_{-h}^{0} \rho g z dz dx = -\rho g \lambda h^2$ the potential energy of the still water level. $E(0)$ is the initial energy budget of the wave and $\gamma = 2\nu k^2$ is the decaying rate, ν being the kinematic viscosity of the fluid. As mentioned, our aim is to evaluate the effect of the resonator on the propagation of the wave for different values of the frequency of the resonator ω_r. If the oscillator were in vacuum or in a low-density fluid, its frequency would simply be given by $\boldsymbol{\omega_r} = \sqrt{\boldsymbol{\kappa}/m}$; however, because of the presence of a dense fluid, a proper evaluation of the latter also needs to account for the added mass given by the surrounding fluid, which results in a frequency $\boldsymbol{\omega_r} = \sqrt{\boldsymbol{\kappa}/(m + \rho_w \mathscr{V})}$, with $\mathscr{V}$ the volume of the resonator.

We start by studying the interaction of a single resonator with the wave. Depending on the ratio Ω, the energy transfer from the wave to the resonator can be more or less effective. The efficiency of the energy transfer from waves to the resonators is more clearly visible in the total energy history of the wave displayed in Fig. 5. The plot shows that small and large values of Ω are associated with smaller dissipation, whereas values of Ω close to unity are more dissipative. In these cases, a large amount of energy is lost in few wave periods. To quantify this effect, we have performed a fit of these curves with an exponential of the form $E(t) \sim E(0) \exp[-Dt]$. The coefficients of the fit are reported in Fig. 6, where we show the results for simulations with up to four resonators. The curves show a clear dissipation peak around $\Omega = 1$. The plots include the results for arrays of fixed cylinders, labeled by $\Omega = 0$. Independently of the number of resonators, we observe a range of frequency ratios, between 0 and 1, for which the dissipation is smaller than for the case of fixed resonators. This dip is particularly evident for the case of one resonator per wavelength and is reduced when the number of cylinders is increased. The dissipation then increases and displays a peak for $\Omega \sim 1$. For $\Omega > 1$, it decreases and appears to approach an asymptote close to the value found for fixed cylinders. It is worth noticing that the curves in Fig. 6 resemble the curves reported for a system for wave energy conversion[18] in which the focus is on maximizing the extracted power. This seems to indicate that the system

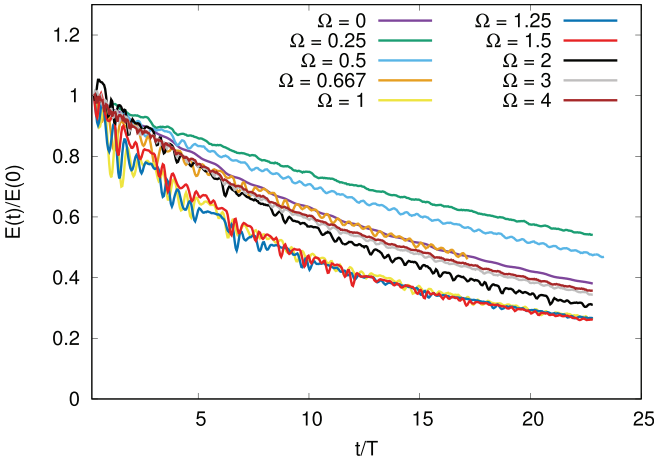

FIG. 5. Time history of the total energy vs the frequency ratio Ω for the case of one single resonator.

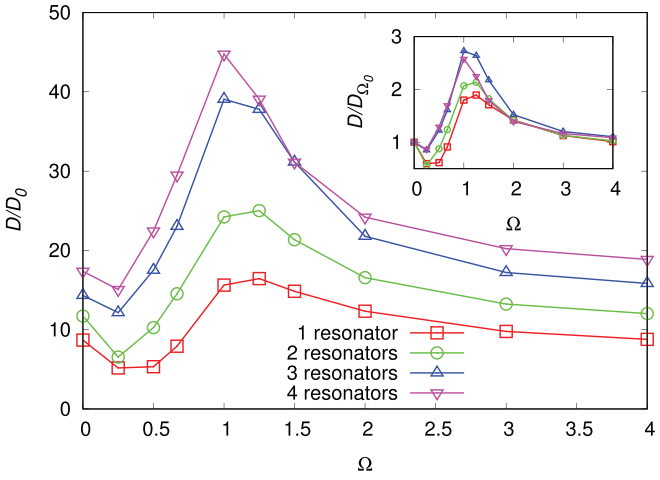

FIG. 6. Dissipation coefficient D normalized with the value for simple traveling wave D_0 vs the frequency ratio Ω for different number of oscillators. In the inset the same data are reported normalized with respect to the dissipation corresponding to the case of fixed cylinders D_{Ω_0} (computed separately for each case).

of submerged resonators is a rather efficient system in dissipating wave power. As the number of resonators is increased, the dissipation also increases. However, this is not a trivial effect due to the total viscous drag of the cylinders on the fluid. Indeed, the ratio between the peak value of the dissipation (around resonance) and the fixed-cylinder value increases as the number of resonator increases between 1 and 3, and appears to decrease with four resonators. This suggests that nontrivial interaction effects are present. It is also interesting to observe that the width of the dissipation peak, and therefore the range of frequencies for which the dissipation is greater than the fixed-obstacle case, becomes wider. Therefore, decreasing the ratio between the wavelength of the wave and the wavelength of the periodic structures enlarges the range of frequencies for which an array of resonators produces a gain in dissipated power with respect to an array of fixed obstacles. An example of the flow field with four resonators and $\Omega = 1$ is reported in Fig. 7. In this case, the characteristic size of the perturbations induced by the resonators on the interface is of the order of the size of the periodic structure. It is worth mentioning that, in the presence of a current, two main effects could be expected: (i) beacuse of the Droppler shift, the frequency of the wave can be shifted with respect to that without a current; this would simply lead to a horizontal shift of Fig. 6; (ii) the current may result in an extra force on the cylinder due to the exchange of the momentum between the current and the resonator. Clearly, if the current is small compared to the velocities induced by the waves, the effect is negligible. However, in the case of strong currents, the cylinder may enter an overdamped regime and may no longer oscillate. Notice that the present model can model the presence of a current, since it can be included in the rhs of (6).

In Fig. 8 we report the time history of the center of mass of the resonators for $\Omega = 1$ and for a different number of resonators. In the case of two oscillators [Fig. 8(b)], the curves have a Pearson correlation index of about -0.94, indicating that the oscillators are in phase opposition, as also clearly shown by the plot. For the case of three oscillators, instead, the correlation indexes of the curves are all about -0.5 because of a phase shift in the motion of the resonators [Fig. 8(c)].

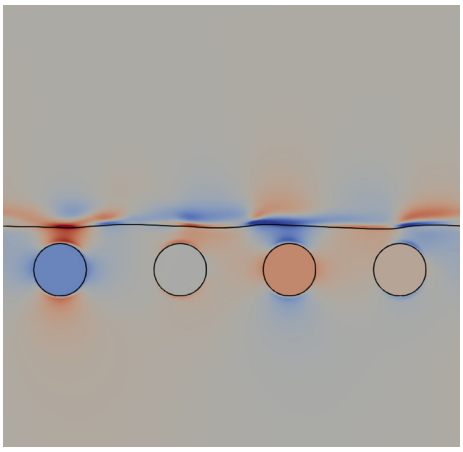

FIG. 7. Snapshots of the horizontal velocity component u, interface location and resonators position for the case with four resonators and $\Omega = 1$ after one wave period. Colors as in Fig. 2 (multimedia view: https://doi.org/10.1063/5.0048613.2).

Finally, in the last case, we find that the oscillators are correlated over a distance equal to $\lambda/2$, since the correlation coefficients for the first and third resonator, as well as that for the second and fourth, are about -0.97, while for the other pairs the coefficient is about 0.1.

IV. CONCLUSIONS

In this work, we have suggested to exploit the concept of mechanical metamaterials in the field of fluid mechanics, using of submerged resonators that interact with traveling waves, absorbing and dissipating mechanical energy. In order to properly describe the behavior of the system, we have simulated the full Navier–Stokes equations for multiphase flows with fluid–structure interaction; this approach allows for a complete and detailed evaluation of hydrodynamic forces acting on the resonators and of the energy dissipation.

We have performed simulations in a periodic square domain of size equal to the wavelength of the wave, varying the elastic force acting on the resonators (i.e., their natural frequency) and the number of resonators per unit wavelength. We have computed the time history of the wave energy and found a dissipation coefficient by fitting the

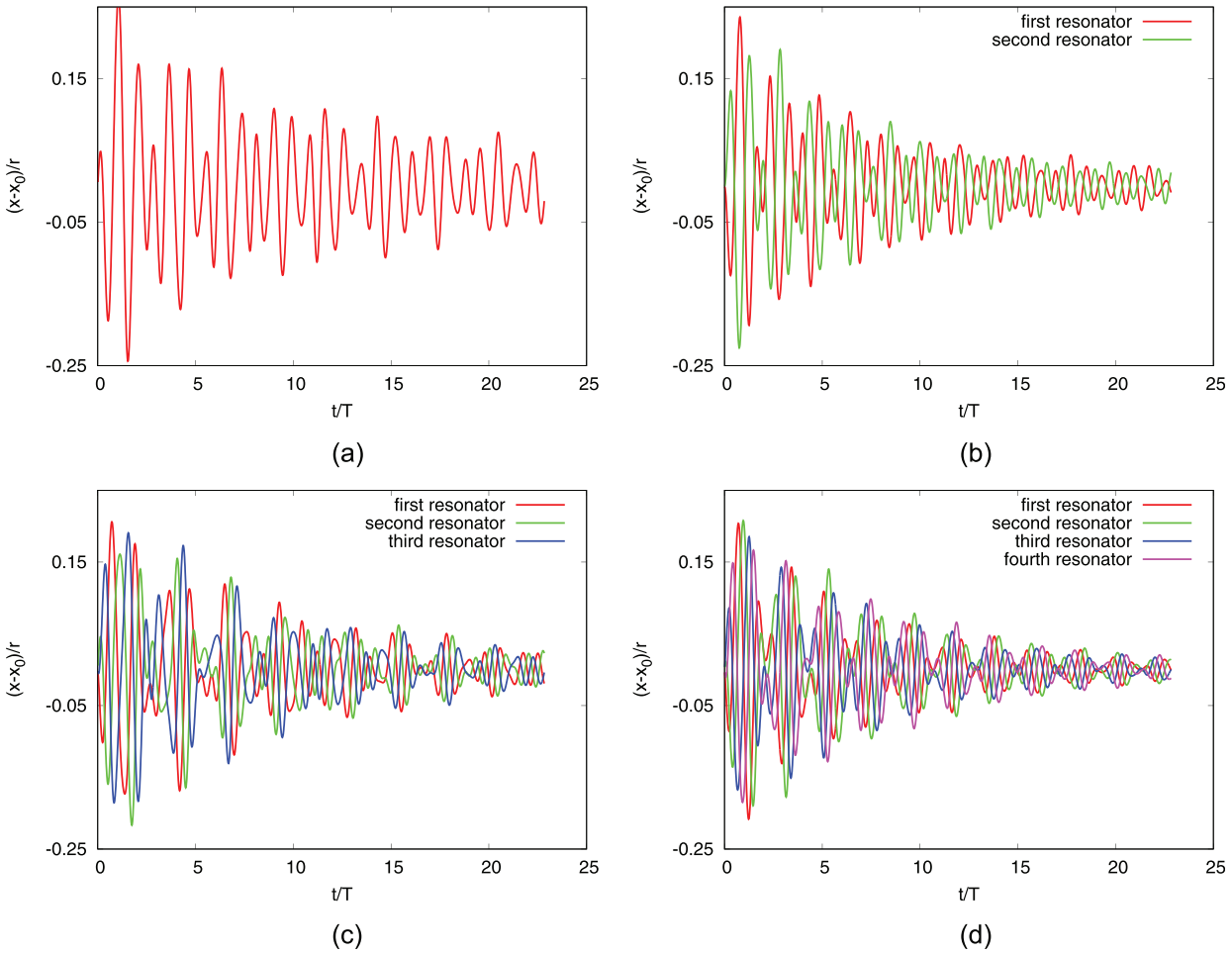

FIG. 8. Time history of the horizontal position of the center of mass of the oscillators: (a) case with 1 resonator (b) case with two resonators; (c) case with three resonators; and (d) case with four resonators. For all cases $\Omega = 1$.

energy decay with an exponential function, similar to that of the viscous dissipation of a simple traveling wave. By doing so, we have found that there is a peak of dissipation when the frequency of the wave and the frequency of the resonators approximately coincide. The dissipation observed at the peak is much larger than that caused by an array of fixed cylinders, so that the width of the peak represents the range for which the oscillatory dynamics (and, possibly, the fluid-mediated interaction among the structures) produces a gain in the dissipated power. Finally, the presence of a dissipation peak centered around a characteristic frequency suggests the presence of a bandgap in the dispersion relations. The width of this bandgap should increase with the number of resonators.

Future work will focus on coupling this system with a numerical wave maker to properly evaluate the dispersion relation and also to investigate the effect of resonator masses on the bandgap. Additionally, the extension of the method to deformable solid bodies could open the field of applications also to flexible underwater structures. This work could open new applicative possibilities to realize low-cost, minimally invasive devices for ocean wave attenuation, contributing to reduced costal erosion or protection of infrastructure such as offshore platforms or harbors.

ACKNOWLEDGMENTS

M. Onorato, F. De Lillo, and F. De Vita have been funded by Progetto di Ricerca d'Ateneo CSTO160004, by the "Departments of Excellence 2018/2022" Grant awarded by the Italian Ministry of Education, University and Research (MIUR) (No. L.232/2016). The authors acknowledge the EU, H2020 FET Open BOHEME Grant No. 863179, the Bando PoC 2019/2021 from Fondazione San Paolo, and CINECA for the computational resources under the grant IscraCSGWA.

DATA AVAILABILITY

The data that support the findings of this study are available from the corresponding author upon reasonable request.

REFERENCES

[1]P. A. Deymier, "Introduction to phononic crystals and acoustic metamaterials," in *Acoustic Metamaterials and Phononic Crystals* (Springer, 2013), pp. 1–12.
[2]M. I. Hussein, M. J. Leamy, and M. Ruzzene, "Dynamics of phononic materials and structures: Historical origins, recent progress, and future outlook," Appl. Mech. Rev. **66**, 040802-1–040802-38 (2014).
[3]J. Pendry, "Electromagnetic materials enter the negative age," Phys. World **14**, 47 (2001).
[4]A. Davies and A. Heathershaw, "Surface-wave propagation over sinusoidally varying topography," J. Fluid Mech. **144**, 419–443 (1984).
[5]T. Hara and C. C. Mei, "Bragg scattering of surface waves by periodic bars: Theory and experiment," J. Fluid Mech. **178**, 221–241 (1987).
[6]X. Hu, Y. Shen, X. Liu, R. Fu, and J. Zi, "Complete band gaps for liquid surface waves propagating over a periodically drilled bottom," Phys. Rev. E **68**, 066308 (2003).
[7]X. Hu, C. Chan, K.-M. Ho, and J. Zi, "Negative effective gravity in water waves by periodic resonator arrays," Phys. Rev. Lett. **106**, 174501 (2011).
[8]P. Kar, T. Sahoo, and M. Meylan, "Bragg scattering of long waves by an array of floating flexible plates in the presence of multiple submerged trenches," Phys. Fluids **32**, 096603 (2020).
[9]A. Zareei and R. Alam, "Cloaking by a floating thin plate," in Proceeding of 31st International Workshop on Water Waves and Floating Bodies, Michigan, USA, 2016, pp. 197–200.
[10]Z. Zhang, G. He, W. Wang, S. Liu, and Z. Wang, "Broadband cloaking of multiple truncated cylinders in water waves using the arrangement defects," Phys. Fluids **32**, 067111 (2020).
[11]C. C. Mei, The *Applied Dynamics of Ocean Surface Waves* (World Scientific, 1989), Vol. 1.
[12]H. Heikkinen, M. J. Lampinen, and J. Böling, "Analytical study of the interaction between waves and cylindrical wave energy converters oscillating in two modes," Renewable Energy **50**, 150–160 (2013).
[13]A. Abbasnia and C. G. Soares, "Fully nonlinear simulation of wave interaction with a cylindrical wave energy converter in a numerical wave tank," Ocean Eng. **152**, 210–222 (2018).
[14]S. Jin, R. J. Patton, and B. Guo, "Viscosity effect on a point absorber wave energy converter hydrodynamics validated by simulation and experiment," Renewable Energy **129**, 500–512 (2018).
[15]Q. Xu, Y. Li, Y. Xia, W. Chen, and F. Gao, "Performance assessments of the fully submerged sphere and cylinder point absorber wave energy converters," Mod. Phys. Lett. B **33**, 1950168 (2019).
[16]Y. Li and Y.-H. Yu, "A synthesis of numerical methods for modeling wave energy converter-point absorbers," Renewable Sustainable Energy Rev. **16**, 4352–4364 (2012).
[17]A. S. Zurkinden, F. Ferri, S. Beatty, J. P. Kofoed, and M. Kramer, "Non-linear numerical modeling and experimental testing of a point absorber wave energy converter," Ocean Eng. **78**, 11–21 (2014).
[18]M. Anbarsooz, M. Passandideh-Fard, and M. Moghiman, "Numerical simulation of a submerged cylindrical wave energy converter," Renewable Energy **64**, 132–143 (2014).
[19]J. Kim and P. Moin, "Application of a fractional-step method to incompressible Navier-Stokes equations," J. Comput. Phys. **59**, 308–323 (1985).
[20]C.-W. Shu, "High order weighted essentially nonoscillatory schemes for convection dominated problems," SIAM Rev. **51**, 82–126 (2009).
[21]E. A. Fadlun, R. Verzicco, P. Orlandi, and J. Mohd-Yusof, "Combined immersed-boundary finite-difference methods for three-dimensional complex flow simulations," J. Comput. Phys. **161**, 35–60 (2000).
[22]R. W. Hamming, "Stable predictor-corrector methods for ordinary differential equations," J. Assoc. Comput. Mach. **6**(1), 37–47 (1959).
[23]F. D. Vita, F. D. Lillo, R. Verzicco, and M. Onorato, "A fully eulerian solver for the simulations of multiphase flows with solid bodies: Application on surface gravity waves," arXiv:2006.05361.
[24]L. D. Landau and E. M. Lifshitz, *Fluid Mechanics* (Pergamon Press, 1959).
[25]K. Zhang, B. C. Douglas, and S. P. Leatherman, "Global warming and coastal erosion," Clim. Change **64**, 41 (2004).
[26]E. C. Bird, *Coastal Geomorphology: An Introduction* (John Wiley & Sons, 2011).
[27]L. Firth, R. Thompson, K. Bohn, M. Abbiati, L. Airoldi, T. Bouma, F. Bozzeda, V. Ceccherelli, M. Colangelo, A. Evans *et al.*, "Between a rock and a hard place: Environmental and engineering considerations when designing coastal defence structures," Coastal Eng. **87**, 122–135 (2014).
[28]F. Bulleri and L. Airoldi, "Artificial marine structures facilitate the spread of a non-indigenous green alga, *Codium fragile* ssp. *tomentosoides*, in the north Adriatic Sea," J. Appl. Ecol. **42**, 1063–1072 (2005).
[29]F. Lalli, A. Bruschi, L. Liberti, V. Pesarino, and P. Bassanini, "Analysis of linear and nonlinear features of a flat plate breakwater with the boundary element method," J. Fluids Struct. **32**, 146–158 (2012).
[30]W. K. Lee and E. Y. Lo, "Surface-penetrating flexible membrane wave barriers of finite draft," Ocean Eng. **29**, 1781–1804 (2002).